Thermal Probe Measurements of the Glass Transition Temperature for Ultrathin Polymer Films as a Function of Thickness

David S. Fryer, Paul F. Nealey, and Juan J. de Pablo*

Department of Chemical Engineering, University of Wisconsin, Madison, Wisconsin 53706

Received February 23, 2000

ABSTRACT: The glass transition temperature of polystyrene and poly(methyl methacrylate) films on polar and nonpolar substrates was measured as a function of thickness using a thermal probe in contact with a polymer film. Using a technique called local thermal analysis, heat loss into the film was monitored as the temperature of the probe was ramped from ambient temperature to temperatures as high as 200 °C. The glass transition temperature was determined from a change in slope in the heat loss versus temperature plot. The T_g of polystyrene on silicon oxide decreased by as much as 25 °C below the bulk value for films 13 nm thick. The same trend in the glass transition temperature was observed for polystyrene films on silicon oxide treated with hexamethyldisilizane (HMDS). The T_g of poly(methyl methacrylate) on silicon oxide increased by up to 7 °C above the bulk value for films 18 nm thick. For poly(methyl methacrylate) on silicon oxide treated with HMDS, the T_g decreased by 10 °C below the bulk value for films 21 nm thick. The glass transition temperatures measured with the thermal probe compared favorably with values of T_g determined by ellipsometry. Local thermal analysis is an alternative to methods of determining T_g based on thermally induced changes in film thickness. The technique, relying on changes in the heat capacity and modulus of the polymer at T_g, may help resolve the current controversies over the measurement of the T_g in thin films.

Introduction

The nature of the transition from liquid to glass and the dynamics of molecular motion in glassy systems are active areas of research.[1] Glasses in the form of thin films, such as thin polymer films, are ubiquitous in industrial applications. For example, thin polymer films (photoresists) are used extensively in semiconductor lithography. The thickness of films used in advanced lithography to form sub-0.1 μm features may be less than 100 nm.[2,3] For polymers used in chemically amplified photoresist, the glass transition temperature is a critical material property. The temperature selected for processing a photoresist film is strongly influenced by proximity to the glass transition temperature. The choice of processing temperature can impact the contrast, resolution,[4] and side-wall roughness[5] of the photoresist.

A central question concerning the glass transition is how molecular motion is arrested in the glassy state to result in very slow dynamics. One postulate is that glasses are dynamically heterogeneous, and motion within them occurs through the correlated motion of large groups of molecules.[6] Probe diffusion measurements that compare the temperature dependence of rotational and translational diffusion indicate that spatially heterogeneous dynamics occur within glasses near the T_g. For *o*-terphenyl, the length scale for heterogeneous dynamics was estimated to be 3 nm.[7] The length scale was larger for polystyrene, on the order of 10 nm.[8] The existence of regions of heterogeneous dynamics within a glass suggests the possibility of a characteristic length scale associated with the glass transition. One method of investigating the length scales of these structures is to observe at which point the dimensions of a system begin to interfere with the length scales associated with the glass transition temperature.

Many researchers have attempted to determine the film thickness at which the T_g differs from the bulk value; the great majority of this research has focused on polystyrene (PS). The results of several experiments, four independent studies, aimed at measuring the T_g in ultrathin PS films, indicate that the T_g of PS decreases below the bulk value at a threshold thickness of approximately 40 nm. Keddie, Jones, and Cory first reported a 27 °C decrease in the T_g of PS on an Si−H substrate for films between 10 and 40 nm in thickness using spectroscopic ellipsometry.[9] Forrest et al. also reported a decrease in T_g for PS films on SiO_x using nulling ellipsometry.[10] Positron annihilation spectroscopy (PALS) measurements of the apparent T_g of PS films on Si−H near the PS−vacuum interface indicated a decrease in the apparent T_g as the film thickness decreased;[11] the results from PALS measurements are consistent with those of ellipsometry. Results from quartz crystal microbalance (QCM) measurements suggest that the T_g of PS on gold substrates decreases with film thickness.[12] Satomi et al. measured the surface molecular motion of polystyrene as a function of molecular weight with scanning viscoelasticity microscopy (SVM).[13] On the basis of measurements of the surface phase lag, they concluded that the local T_g at the surface is lower than for the bulk and that it decreases with molecular weight even in relatively thick films (e.g., 200 nm). X-ray reflectivity measurements also indicate that the T_g of PS departs from the bulk value in ultrathin films; surprisingly, however, these measurements found that T_g *increases*. Using X-ray reflectivity to measure T_g, Wallace et al. reported an increase in T_g for PS films on an Si−H substrate. (The glass transition, during temperature ramps up to T_g + 60 °C, was not observed in films less than 50 nm thick.[14])

In addition to measurements of T_g, several studies of polymer mobility suggest that the T_g of a polystyrene film either decreases or increases with decreasing film

10.1021/ma0003349 CCC: $19.00
Published on Web 07/29/2000

thickness. Using fluorescence recovery after patterned photobleaching, Frank et al. measured slower PS chain diffusion relative to the bulk in films thinner than 150 nm.[15] They concluded that the observed effects could not be explained solely on the basis of a decrease in the T_g of polystyrene. On the basis of measurements of the diffusion of deuterated polystyrene into hydrogenated polystyrene, Zheng et al. reported results similar to those of Frank et al.; i.e., diffusion was slower in thin films than in thicker films.[16] The authors suggested that an "effective" T_g of PS that increases by 25 °C as the thickness decreased from 188.2 to 7.6 nm could be invoked to explain the observed slowing down of diffusion. Using photon correlation spectroscopy and quartz crystal microbalance techniques, Forrest et al. showed that the relaxation dynamics of polystyrene shift to a lower temperature in thinner films, consistent with a decrease in T_g in thin films of polystyrene.[12]

Similar to the work with polystyrene, studies have been conducted to investigate thin film effects on the T_g in polar polymers such as poly(methyl methacrylate) (PMMA). Keddie et al. reported spectroscopic ellipsometry measurements of the T_g of PMMA, indicating that the T_g increases by 5 °C on SiO_x but decreases by 15 °C on gold in films less than 40 nm thick.[17] However, Kahle et al. have recently reported spectroscopic ellipsometry measurements indicating that the T_g for PMMA films cast on SiO_x for films as thin as 20 nm does not change appreciably from the bulk value.[18] The discrepancy between the results was attributed to the temperature dependence of the substrate optical properties.

Several authors have attempted to explain the effect of film thickness on the glass transition temperature theoretically. Jiang et al. proposed a model employing an analogy between the glass transition and the melting transition.[19] The model utilized the concept of correlation length and other thermodynamic properties (heat capacity, mean-square distance between molecules) to qualitatively describe finite-size effects on T_g without a need for adjustable parameters; however, it only predicts a decrease in T_g. Forrest et al. have recently proposed a multilayer model to describe all the effects of film thickness on T_g in polystyrene.[20] The model is based on incorporating the ideas of a length scale for cooperative dynamics by representing the polymer film with interfacial layers of higher or lower mobility and assigning an effective glass transition temperature to each layer. The model is capable of quantitatively reproducing most of the polystyrene results reported in the literature, including an increase in T_g with film thickness. Torres et al. have also anticipated many of the experimental results from the literature using molecular dynamics simulations.[21] By changing the intermolecular potentials acting between the polymer segments and the interface, the simulations reveal the existence of low or high mobility layers near the substrate or near the air interface, and they capture the thin film behavior of T_g for both supported and freely standing films. We propose using interfacial energy to unify the observed effects of film thickness on T_g.[22] Note, however, that despite theoretical interest in this problem, several experimental issues must still be resolved; these issues have led to some inconsistencies in published work in this area.

Given the disagreement in the literature, possibly caused by limitations in the experimental techniques or from comparing disparate phenomena, and in view of the prevailing incomplete picture of polymer−substrate effects on T_g, it is of interest to conduct a new study with a novel and different method of measuring the T_g in polymer films on well-characterized surfaces. In this paper, we report measurements of T_g in thin films based on local thermal analysis. The technique detects the T_g by measuring changes in the heat flow from a $1\ \mu m \times 0.25\ \mu m$ area heat source in contact with a polymer film. In the experiment, a hot probe is brought into contact with a polymer film cast on a substrate. The substrate acts as a heat sink. The power required to keep the probe at a temperature set point is measured. The temperature set point is ramped from ambient temperature to temperatures greater than the T_g. At the T_g, there is an increase in power supplied to the probe. The origin of the response is attributed to a change in the heat capacity and the modulus of the polymer film. The experiment measures the T_g near the surface of a polymer film as a result of temperature gradients introduced by the heat source. The origin of the signal and the temperature profiles in the film are considered at length in the discussion. Films as thin as 10−20 nm were investigated with the technique. We report local thermal analysis measurements of T_g as a function of thickness in polystyrene and PMMA on both polar (SiO_x) substrates and nonpolar (SiO_x treated with a surface agent, hexamethydisilizane) substrates. For purposes of comparison, measurements of the T_g of thin films using ellipsometry are also reported.

Experimental Section

Materials. Polystyrene (PS) ($M_w = 382 \times 10^3$ g/mol, $M_w/M_n = 1.16$) was purchased from Aldrich (Milwaukee, WI). Poly(methyl methacrylate) (PMMA) ($M_w = 100 \times 10^3$ g/mol, $M_w/M_n = 1.03$) was purchased from Polysciences, Inc. (Warrington, PA). Poly(4-hydroxystyrene) (PHS) ($M_w = 10.8 \times 10^3$ g/mol, $M_w/M_n = 2$) was provided by Hoechst Celanese (Corpus Christi, TX). Poly(phenol formaldehyde) (novolak) ($M_w = 9.33 \times 10^3$ g/mol, $M_w/M_n \sim 5$) was provided by Schenectady International (Schenectady, NY). SAL605, a photoresist based on novolak, and Apex-E, a photoresist based on PHS, were provided by Shipley (Marlboro, MA). Toluene, propylene glycol methyl ether acetate (PGMEA), hexamethyldisilizane (HMDS), hexacosane (C_{24}), hexatriacontane (C_{36}), tetratetracontane (C_{44}), pentacontane (C_{50}), and hexacontane (C_{60}) were purchased from Aldrich (Milwaukee, WI). Silicon wafers (100 orientation) were obtained from III TYGH.

Sample Preparation. Silicon wafers were immersed in a solution of sulfuric acid and hydrogen peroxide (95:05 ratio by volume) for 1 h and washed with distilled water to remove any organic material from the surface. Nonpolar surfaces were prepared by placing the silicon substrates in an atmosphere of HMDS in a vacuum oven (Yield Engineering Systems) at 147 °C and 5 Torr pressure for 5 min. The water contact angle (Rame-Hart goniometer) on the HMDS covered surface was approximately 70−80° for 5 min exposure time.

The photoresist films, SAL605 and Apex-E, were prepared by spin-casting (3000 rpm) with a coater (Solitec) on silicon treated with HMDS. The films were processed (post-apply bake on a vacuum hot plate: 110 °C/60 s for SAL605, 90 °C/60 s for Apex-E) according to the conditions optimized for X-ray exposure to form 550−600 nm films. Novolak (10% by mass) and PHS (15% by mass) were dissolved in PGMEA and spin-cast (2000 rpm) to form films 250 and 650 nm thick, respectively, after annealing. The films were annealed for 12 h in an Imperial IV convection oven (Lab Line Instruments, Inc.) at 120 °C (for novolak) and 180 °C (for PHS) with 1−2 °C/min ramp to cool. PS and PMMA films were prepared by spin-casting (2000 rpm) from a solvent of toluene (0.1 μm filtered) with concentrations ranging from 0.6% to 2.3% by mass. The

polymer films were annealed at 20−40 °C above the bulk T_g for 12 h in a vacuum oven (VWR Scientific) and allowed to cool to room temperature at ~1 °C/min to produce samples with a well-defined and reproducible thermal history.

Surface Roughness Measurements. The rms roughness of the PS and PMMA films was measured with noncontact scanning probe microscopy using a Thermomicroscopes Voyager system (Santa Clara, CA) equipped with an Explorer scanning head. Noncontact scanning probes were characterized with NT-MDT AFM gratings. The silicon nitride probes each had approximately 20 nm tip radii. The measured rms roughness of the surface of the polymer films was less than 10 Å.

Ellipsometry Thickness Measurements. The thickness of the films was determined using an Auto EL nulling ellipsometer (Rudolph) at three wavelengths: 632.8, 546, and 405 nm. The angle of incidence of the beam was 70° to the sample. The resolution of the instrument was ±0.04° in Δ and Ψ. The values of the thickness were determined using FilmEllipse software version 1.1 (Scientific Company, Intl.) from all three values of Δ and Ψ. The thickness of the native oxide layer of the silicon wafers was determined by ellipsometry to be 9−15 Å.

Ellipsometry T_g Measurements. The polymer samples were placed on a hot plate (Reichert-Jung) mounted on the optical stage of the ellipsometer. The temperature was ramped at 3−5 °C/min by manually resetting the constant temperature controller. The temperature ramp using this method was linear in time. A least-squares fit of the temperature with time typically yielded $R^2 \geq 0.998$. The surface temperature of the silicon wafer on the hot plate stage was calibrated to a thermometer inset using the melt transition of long chain alkanes. Five alkanes were melted to the wafer surface at high temperature, then cooled, and reheated to record the melt transition and corresponding thermometer reading. By visually observing the consecutive melting points for five waxes (C_{24}, C_{36}, C_{44}, C_{50}, and C_{60}) at a ramp rate of 1 °C/min, the thermometer was calibrated within an accuracy of ±0.5 °C.

Ellipsometry measurements were taken every 30−40 s during the temperature ramp. For thicker films, the T_g was determined using any of the three wavelengths. For thin films of PS and PMMA the values of the T_g were detected by analyzing data from the wavelength and Δ or Ψ value that was the most sensitive to changes in thickness with temperature. In all cases, the most sensitive wavelength was 405 nm and Ψ was consistently more sensitive than Δ. The T_g was determined from the intersection of the best fit of two straight lines to the data over the temperature range of the experiment as described in the literature.[9]

Local Thermal Analysis. The scanning thermal microscope used in the study was a Thermomicroscopes Voyager instrument equipped with an Explorer scanning head. The thermal control unit (TCU) and thermal probes were also purchased from Thermomicroscopes. The thermal control unit is a dc mode instrument; all feedback voltages and thus the temperature ramp applied to the thermal probe were dc.

Differential Scanning Calorimetry. The glass transition temperature of the bulk polymers was measured with a Netzsch differential scanning calorimeter (DSC). Ramp rates used in the DSC were set to match the ramp rates used with ellipsometry and local thermal analysis for comparison purposes. The ramp rates varied from 3 to 5 °C/min.

Results

Figure 1 shows a schematic representation of the setup for the local thermal analysis experiment. The diagram shows the two main parts of the experimental design: the thermal control unit (TCU) and a remotely connected microresistive element or thermal probe. The TCU is a Wheatstone bridge circuit, with a feedback loop, that supplies power to the probe to maintain it at a constant temperature. The thermal probe is a thermistor element mounted on a scanning probe microscope (SPM) head that changes resistance with small changes in current. The temperature of the thermal probe is a linear function of the resistance. During an experiment, the power supplied to the probe to keep the temperature at a set point is measured. The temperature set point is ramped from ambient temperature to temperatures greater than the T_g. The T_g appears as a change in the slope of power supplied to maintain a temperature set point as a function of the probe temperature. The thermal probe itself is the central part of the experimental design and controls the sensitivity of the technique.

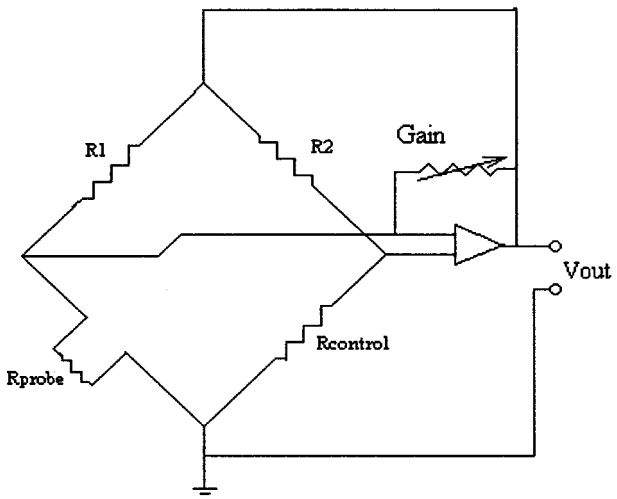

Figure 1. Diagram of the Wheatstone bridge circuit used to heat the resistive probe and record heat flows from the probe into the sample. The controlling resistance ($R_{control}$) and probe resistance (R_{probe}) are held at a constant ratio of R_2/R_1 by the feedback loop.

Figure 2 shows a diagram of the thermal probe resistor and an SEM micrograph of the probe. The probe is a platinum/10% rhodium alloy that is 5 μm in diameter and 200 μm in length. The probe surface is somewhat rough and curved, such that only a small cross section of the probe diameter is in contact with the sample surface during measurement. The legs of the thermal probe resistor that form the cantilever of the probe have a mirror attached for use in standard SPM operation, such as monitoring the height or force of the probe on the sample.

Figure 3 shows plots of the calibration of the resistance of the thermal probe to temperature. The temperature coefficient of resistance of the thermal probe material is known ($\alpha = 0.001\ 65\ K^{-1}$). By determining the exact resistance of the probe at a known temperature, the entire range of temperature versus resistance behavior can be determined. The calibration temperature used was the melt transition temperature of long chain alkanes. The plots show the power output to the probe as a function of resistance while the probe was in contact with a hard, waxy solid, hextriacontane (C_{36}, $T_m = 72$ °C). The heat flow data in Figure 3a are calculated from the difference in power supplied to the probe while it was out of direct contact with the sample (in air) and the power supplied to the probe while in direct contact with the sample at each setting of probe resistance. By subtracting the heat flow data, only heat transfer by conduction at the contact point is represented in the plot. Below the melt transition, heat flow at the probe−sample contact point gradually increases with a slope of approximately 200−300 mW/ohm. At the melt transition, the power supplied to the probe

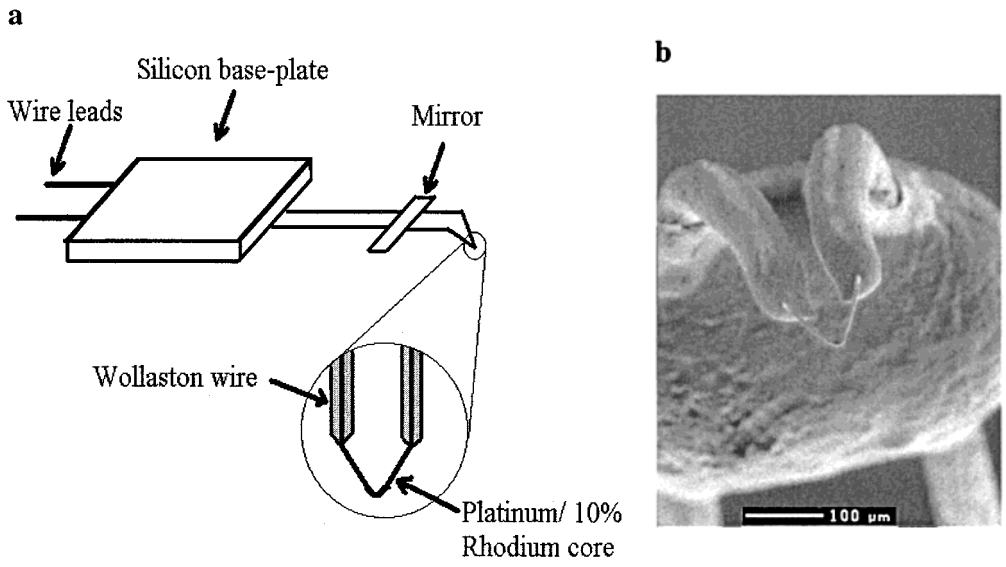

Figure 2. (a) Diagram of the thermal probe that forms the probe resistance of the Wheatstone bridge. The Wollaston process wire is silver; the wire is attached to a silicon die for mounting on the scanning probe microscope head. (b) A SEM micrograph of the tip of the probe; the exposed wire is a thermistor material that is platinum/10% rhodium in composition. In the background is an image of the epoxy glue that holds the legs of the Wollaston wire together.

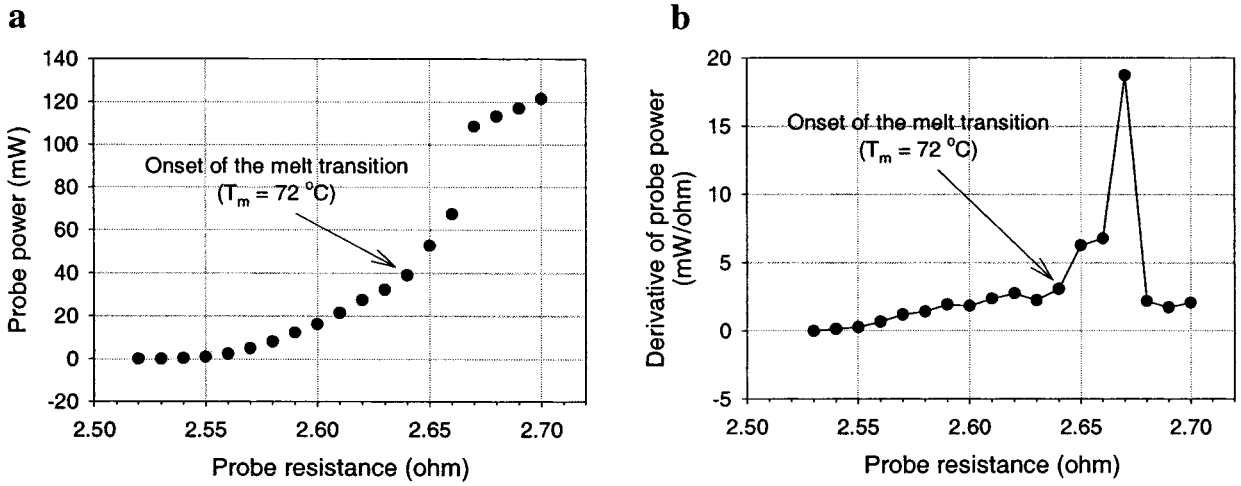

Figure 3. (a) Plot of the power supplied to the probe as a function of the probe resistance for the probe in contact with hexatriacontane (C_{36}). The power was calculated from the feedback of the Wheatstone bridge circuit. (b) Plot of the derivative of the probe power as a function of probe resistance. The onset of the melt transition was detected at 2.64 ohms.

increases from 35 to 105 mW over 0.5 ohms (12.5 °C). The melt transition that appears as a gradual change in slope in Figure 3a appears as a peak in a plot of the derivative of power versus resistance in Figure 3b. The value of the resistance at the onset of the change in signal was more reproducible than the resistance at the peak. As discussed later, the behavior of the signal after the initial increase at the phase transition is a measure of the change in contact area between the probe and sample. The contact area, after the initial increase in signal, changes between measurements and can shift the peak in the temperature scan. Thus, the onset of the increase in signal was used to calibrate the probe resistance to temperature. As in the calibration analysis discussed above, phases transition temperatures, T_m and T_g, were inferred from the derivative of the thermal analysis data.

Figure 4 shows a plot of a measurement of the glass transition temperature on a polystyrene film with the thermal probe. The plot shows a thermal scan on a 85 nm film of polystyrene cast on a SiO_x substrate treated with HMDS. The heat flow as a function of temperature has a region of constant slope at low temperatures. The low-temperature segment of the scan is followed by another segment of increasing heat flow with temperature. The intercept of the two segments corresponds to the bulk value of the glass transition temperature (~102 °C). The clearest intercepts between the temperature segments were those with the least scatter below T_g. The scatter in the thermal data for the low-temperature segment was a function of temperature fluctuations in the ambient temperature of the SPM enclosure, time lag between the air and sample scans, and the quality of the spin of the polymer film (no pinholes and low roughness). Careful control of these conditions offered the best results. The values of T_g reported in this paper were considered acceptable if the variation in the value of T_g was less than ±3 °C based on a 95% confidence interval in a least-squares fit of the data. Generally, this restriction equated to a correlation coefficient of $R^2 \geq 0.98$ for the fit of the data in each temperature segment. The resolution of the

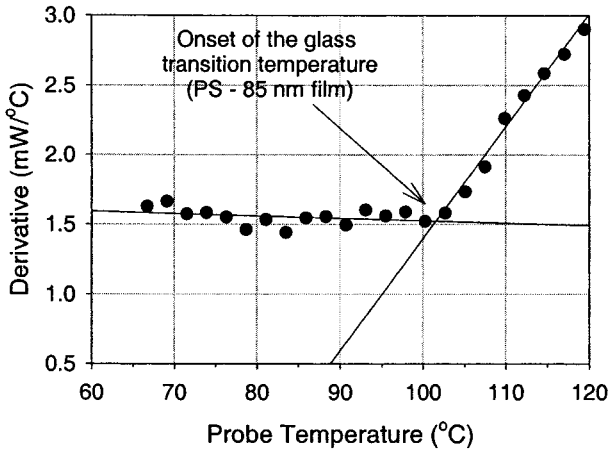

Figure 4. Plot of the derivative of probe power as a function of probe temperature. The polymer film was polystyrene (85 nm thick) on a SiO_x substrate treated with hexamethyldisilizane.

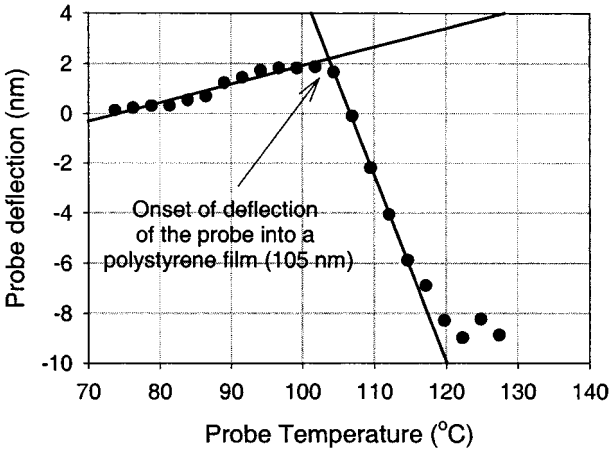

Figure 5. Plot of the probe deflection as a function of the temperature of the probe. The sample was a polystyrene film cast on SiO_x substrate with HMDS. The film was 105 nm thick.

technique is limited by the size of the temperature step, which is ±2.3−2.6 °C. The behavior of the heat flow data with temperature was consistent between measurements and yielded reproducible (within ±3 °C) polystyrene T_g's.

Figure 5 shows a plot of the change in the probe height (indicated by changes in the deflection of the cantilever) on the sample surface during a temperature ramp. Similar to the heat flow data, there are two temperature segments. Initially, there is a small (1−2 nm) deflection away from the film over 40 °C due to thermal expansion in the film and the probe itself. Then there is a steep (10 nm) deflection toward the film below the initial position for the next 30 °C, suggesting the probe has penetrated the sample film. Note that the temperature at which the probe penetrates the film occurs at a temperature increment just after the T_g of polystyrene. The temperature lag between the increase in heat flow at T_g and the probe deflection is consistent between measurements. The force constant of the thermal probe cantilever is ∼5 N/m. We estimate that the force of the probe on the film surface for this measurement was ∼200 nN (which is a force per unit area of $\sim 7 \times 10^5$ N/m^2 based on contact area estimates presented in the following section). The range of forces applied by the probe (50−500 nN) did not influence the measured value of T_g. The dependence of the T_g in polymers on pressure is small[23] and has been reported as $dT_g/dP = 2.5 \times 10^{-7}$ °C/Pa for polystyrene,[24] which translates into a change in T_g of less than ±0.1 °C over the range of forces applied by the probe tip.

Figure 6 shows topography data from an SPM scan of the probe−sample contact area in a polystyrene film after measuring the T_g ($T_{probe} = T_g + 20$ °C). The impression is approximately 10 nm deep and consistent with the change in probe height during the measurement. The results indicate that the area of contact is approximately rectangular, with dimensions (after the probe deflects into the sample) of 1.12 μm by 0.24 μm, or 0.27 μm^2.

Table 1 shows the results from measurements of the T_g in six different polymers and two polymer composites (photoresists). The results agree with differential scanning calorimetry, values from the literature,[25,26] and ellipsometry to within ±5 °C. The data show that the technique yields accurate values of T_g on many different polymers over a large range of glass transition temperatures (a range of about 90 °C).

Figure 7 shows the measured T_g of polystyrene on two substrates, SiO_x and SiO_x with HMDS, as a function of film thickness. For thick films, the thermal probe temperature at which the T_g was detected was the same (±3 °C) as the bulk value. For films less than 45 nm thick, the T_g deviates from the bulk value, decreasing monotonically. The maximum decrease in the T_g, 25 °C below the bulk value, was measured in the thinnest film. Note that for these systems a dependence of the T_g on the substrate is not apparent; there is no significant evidence of differences for a polar or nonpolar substrate. The values of T_g measured with local thermal analysis for PS on SiO_x agree with those measured by ellipsometry.[10] Figure 7 also shows a plot of the measured values of the T_g of polystyrene on a substrate of SiO_x with HMDS, using ellipsometry, as a function of film thickness. The values of T_g for thicker films differ only slightly between the two measurements, approximately 2 °C, which is within the error of each experiment. Both the trend and magnitude of the change in the T_g of polystyrene with thickness are comparable for the two measurements.

Table 1. Results Comparing the T_g Values (in °C) Measured with Local Thermal Analysis to Ellipsometry, DSC, and the Literature

	bulk measurement of T_g (from DSC or literature source)	nulling ellipsometer (thick film > 200 nm)	local thermal analysis (thick film > 200 nm)
poly (methyl methacrylate) atactic, M_w = 100 kg/mol	120.0 ± 1.4	118.0 ± 3.0	119.7 ± 2.5
poly (methyl methacrylate) isotactic, M_w = 27.8 kg/mol	56 ± 3	53.8 ± 3	57.0 ± 2.6
polystyrene, M_w = 382.1 kg/mol	102.6 ± 1.2	99.3 ± 1.5	102.5 ± 2.8
polystyrene, M_w = 44.0 kg/mol	96 ± 2	96.7 ± 3	94.7 ± 2.6
poly(4-hydroxystyrene) (PHS), M_w = 10.8 kg/mol	148.4 ± 3.0	148.3 ± 3.4	149.2 ± 3.4
poly (phenol formaldehyde) (novolak), M_w = 9 kg/mol	90.3 ± 1.3	90 ± 3	88.7 ± 2.8
Apex-E photoresist (based on PHS)	120[24]	119 ± 3	120 ± 2.5
SAL605 photoresist (based on Novolak)	75[25]	74 ± 2	75 ± 2.5

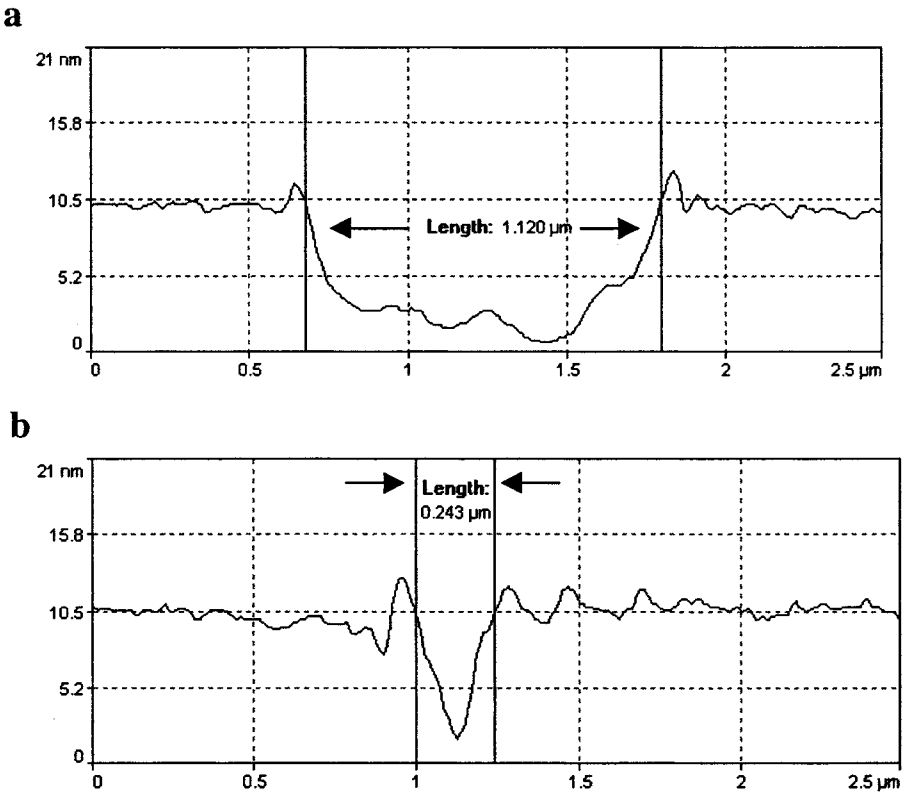

Figure 6. Topography data from a noncontact image of the impression left in a 105 nm polystyrene film after a temperature ramp ($T_{probe} = T_g + 20$ °C) with the thermal probe. (a) Plot of the topography measured with SPM of the impression parallel to probe contact. (b) Plot of topography measured with SPM of the impression perpendicular to probe contact.

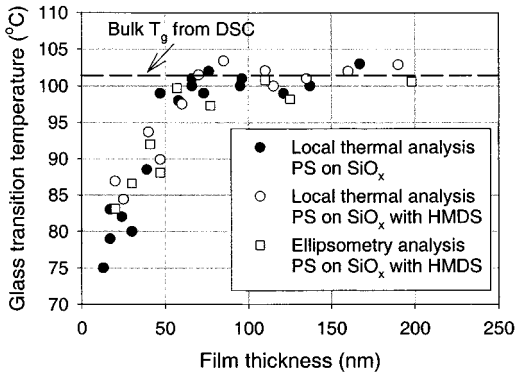

Figure 7. Plot of the results from local thermal analysis and ellipsometry measurements of the T_g of polystyrene films (M_w = 382.1 kg/mol) on substrates of SiO_x and SiO_x with HMDS.

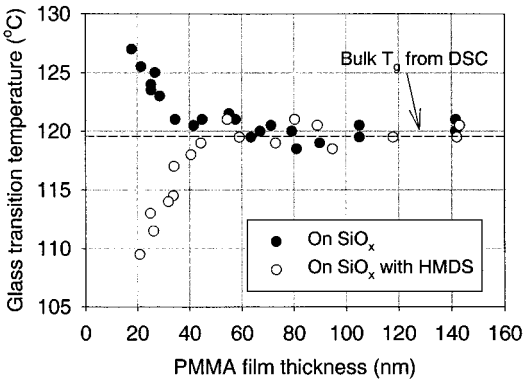

Figure 8. Plot of the results from local thermal analysis measurements of the T_g of poly(methyl methacrylate) films (M_w = 100.3 kg/mol) on substrates of SiO_x and SiO_x with HMDS.

Figure 8 is a plot of the measured values of the T_g of PMMA on two substrates, SiO_x and SiO_x with HMDS, as a function of film thickness. Thick films approach a constant bulk value, within ±3 °C, as measured by differential scanning calorimetry. For thinner films less than 40 nm thick, the T_g begins to deviate from the bulk glass transition temperature. For PMMA films there was a distinct difference in dependence of T_g on film thickness between the two substrates. The T_g increases to a maximum of 7 °C above T_g for films on a substrate of SiO_x. The T_g decreases on the nonpolar substrate of HMDS on SiO_x to a maximum of 10 °C below the bulk T_g. Note that, for PMMA films on SiO_x with a layer of HMDS, the decrease in T_g is less (∼10 °C) than the decrease measured in PS films.

Figure 9 is a plot of the measured values of the T_g of PMMA on SiO_x using two techniques, local thermal analysis and ellipsometry, as a function of film thickness. Both techniques agree over the range of film thickness studied to within the error in each experiment. The ellipsometry results also agree with previously reported trends in T_g measured for PMMA on SiO_x.[17]

Discussion

In an experiment with local thermal analysis, the T_g is determined from an increase in the slope of the heat loss versus temperature data. There are three properties of polymers that could produce this response: an increase in thermal conductivity (k) and heat capacity or a decrease in the (shear) modulus or rigidity of the polymer. We summarize here the relative contributions to the signal at T_g from each of these properties.

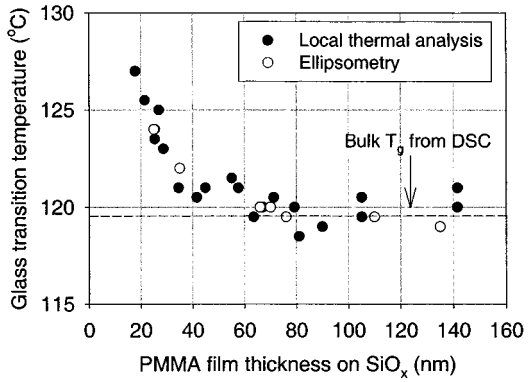

Figure 9. Plot comparing the results from local thermal analysis to results using ellipsometry on the same system, PMMA films on a substrate of silicon oxide.

An increase in the thermal conductivity of the polymer film at T_g is an intuitively appealing origin for the signal, but literature data on the bulk thermal conductivity do not support this conclusion. Measurements of the power supplied to the probe as a function of distance from the film indicate that greater than 75% of the heat transfer is by heat conduction at the probe−sample contact (a result also observed by Gomes et al.[27]). However, changes in bulk thermal conductivity of amorphous polymers at the T_g are relatively small. In fact, *k decreases* with increasing temperature above T_g for many polymers.[28]

The heat capacity increases dramatically in polymers at the T_g, which could influence the signal in local thermal analysis. An increase in the heat capacity is the primary method of identifying the T_g with differential scanning calorimetry (DSC) and modulated DSC. But local thermal analysis differs greatly from DSC experiments in the method of heating the sample. In a typical experiment, the power supplied to the probe below T_g does not change with time after approximately 0.5 s. The TCU records a signal for 20−30 s at each temperature increment. Thus, steady-state heat flow between the probe and sample is probably established. The magnitude of steady-state heat flow from a constant temperature source to a heat sink is governed by the thermal conductivity, not the heat capacity.[29] Note, however, that the power supplied to the probe does change over time at and above the T_g. The power supplied to the probe can change by 5−10 mW during a 20−30 s period. The heat capacity is a factor in time-dependent heat flow. Thus, part of the signal detected in our measurements can be attributed to changes in the heat capacity.

Perhaps the most important source of the change in thermal signal at T_g is from an increase in the contact area between the probe and sample. The probe penetrates the sample during the measurement (see Figures 5 and 6). Concurrently, the shear modulus of the polymer decreases by 4 orders of magnitude, from 10^9 to 10^5 N/m^2, at the T_g.[28] Probe penetration is presumably the result of the film becoming rubbery at the glass transition temperature and unable to support the force applied by the probe at the point of contact. The increase in the thermal signal prior to the probe deflection into the film could be caused by increased contact (wetting of the probe) prior to deformation. Note that repeated temperature scans (heating and cooling and heating again) at the same location yield T_g values within ±2.5 °C of each other (i.e., within the resolution of the technique). The increase in differential power at T_g is smaller in the subsequent scans by approximately 0.5−1.0 mW/°C. This result suggests that the mechanism for detection of T_g arises not only from a change in contact area but also from changes in the thermal properties of the polymer in the melt versus the glassy state.

A remarkable result from this study is the fact that the dependence of the T_g on film thickness is the same whether it is measured with local thermal analysis or ellipsometry. The similarity in results is surprising considering the significant difference in the method of heating the sample with local thermal analysis. Only in the region immediately below probe contact do the heat capacity and modulus of the polymer change at T_g. The thermal probe is an isolated heat source in contact with a heat sink (the polymer film and wafer); therefore, there is a steep temperature gradient in the film. The temperature gradients in local thermal analysis contrast with ellipsometry, which relies on uniform heating of the film. In the following discussion we examine the temperature gradients in the film through mathematical modeling.

Simple mathematical models have been proposed to describe the heat transfer present in ac thermal microscopy;[30,31] however, no models have been proposed that describe the heat transfer in dc thermal analysis. We use a simple analytical model of heat transfer from the probe based on the Laplace equation to study the temperature profile in the sample during the experiment. In the model, all heat transfer is assumed to occur by conduction. Thermal conductivity, k, is assumed constant over the temperature range of the experiment. The thermal conductivities of the materials used are k_{PS} (0.11 W/m/K),[32] k_{PMMA} (0.19 W/m/K),[32] and $k_{silicon}$ (140 W/m/K);[33] these do not vary significantly (∼15% for k_{PS} and k_{PMMA}, less than 5% for $k_{silicon}$) with temperature over the temperature range studied. The approximately rectangular shape of the probe contact (5 × width = length) suggests simplifying the heat flow description by adapting a two-dimensional heat transfer model. The assumption will represent three-dimensional heat transfer to a fair approximation if the heat flux at the edges is similar to that at the center of the probe. As will be demonstrated in the calculation, the approximation introduces only a small error in the resulting temperature profiles. We therefore write, at steady state,

$$\frac{\partial^2 T}{\partial x^2} + \frac{\partial^2 T}{\partial z^2} = 0 \qquad (1)$$

Equations 2−4 describe the boundary conditions of the model.

$$k_{\text{polymer}}\left(\frac{\mathrm{d}T_{\text{polymer}}}{\mathrm{d}z}\right) = k_{\text{silicon}}\left(\frac{\mathrm{d}T_{\text{silicon}}}{\mathrm{d}z}\right) \qquad (2)$$

$$T_{\text{surface}} = T_{\text{ambient}} \qquad \text{for } x < -x_{\text{probe}} \text{ and } x > x_{\text{probe}} \qquad (3)$$

$$T_{\text{surface}} = T_{\text{probe}} \qquad \text{for } x > -x_{\text{probe}} \text{ and } x < x_{\text{probe}} \qquad (4)$$

The assumption of constant flux is used at the interface between the polymer and silicon substrate. At the interface between the probe and film surface, the probe contact is represented by a step function. Finally, the

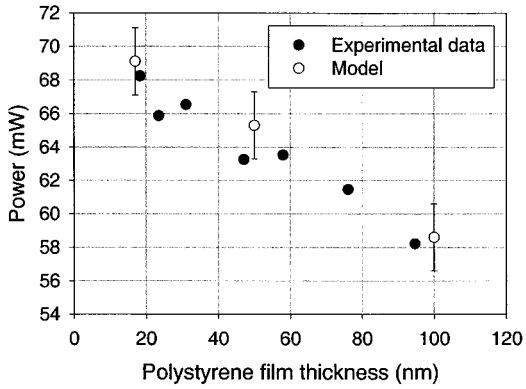

Figure 10. Plot of the fit of the heat flow from the model to experimental data collected on polystyrene for different values of the film thickness. The experiment and model data were determined for a probe temperature of 72 °C.

boundary conditions at the edge of the model film and substrate are constant (ambient) temperature.

Figure 10 shows a plot of the model fit to experimental results of probe heat flow as a function of polymer film thickness. The adjustable parameter in the equation is the size of the probe. Trial calculations were performed to ensure that the size of the probe relative to the size of the model film and substrate did not influence the heat flow values. The error introduced by the assumption of two-dimensional heat transfer is also calculated by varying the area of the probe contact. The equivalent contact area of the probe derived from the calculation was 0.2 μm^2. The model result is in reasonable agreement with the contact area measured with noncontact scanning probe microscopy (0.27 μm^2, Figure 6). The calculated area is less than the measured area because of the inherently higher potential for heat transfer using the geometry in the model (rectangular with solid contact over the entire area of the probe) compared to the actual geometry of the probe contact (ellipsoid with many microcontact points). In addition, the spot measured with SPM is the indentation area after the probe penetrates the film. Given the radius of the curvature of the probe, the measured indentation might exceed the actual contact area between the probe and the film prior to the glass transition. Thus, the difference in the contact area estimated from the model and from experiment is reasonable.

Figure 11 shows a plot of the calculated temperature gradient in a polystyrene film as a function of distance from the probe. The model predicts that the heat flow does not broaden greatly in the film; the heated volume is directly below the probe−sample contact. We can estimate the volume of the film that is measured at the glass transition temperature from the temperature profile. Since the probe temperature is ramped at approximately 2.5 °C intervals, a 5 °C gradient in the film is a reasonable estimate of the region where the glass transition is first measured. On the basis of the heat transfer calculation, approximately 10% of the film near the surface contributes to the signal at the glass transition. The model predicts that the fraction (∼1/10) of the polymer film within 5 °C of the probe temperature at T_g does not vary significantly with thickness. This invariance in the temperature gradient with film thickness is a result of the silicon substrate acting as a heat sink. As a result of high heat flux at the polymer−substrate interface, the temperature at the interface is maintained at ambient. The effect contributes to the

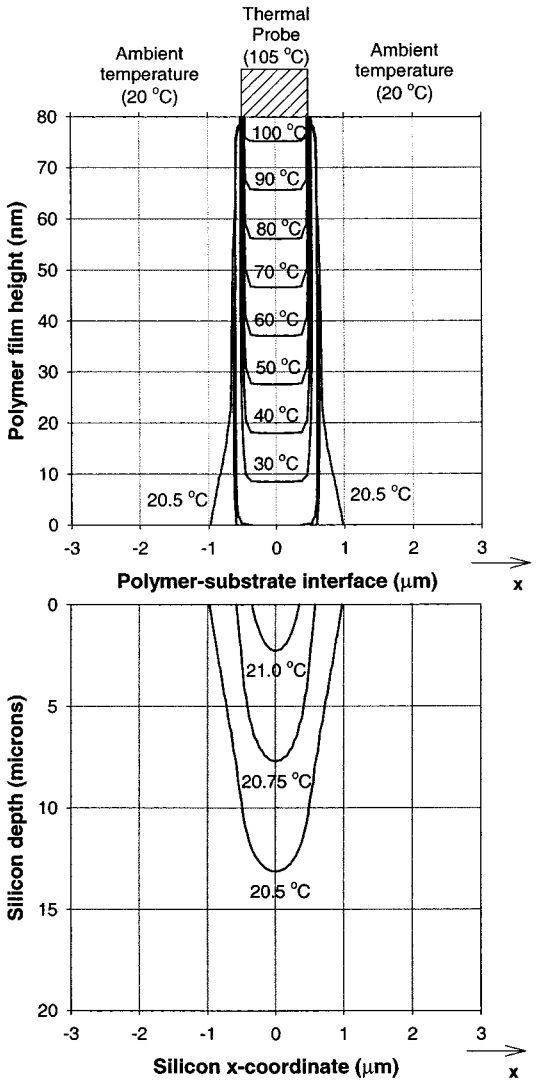

Figure 11. Plot of the calculated temperature gradient in a polystyrene film and in the underlying silicon substrate as a function of distance from the probe. The model prediction is for a thermal probe at 105 °C in contact with an 80 nm thick film. The width of the probe in the calculation was 1.10 μm (i.e., $x_{probe} = 0.55$ μm).

relatively constant (∼10%) volume of the film measured at the T_g independent of the film thickness.

It is possible to interpret the local thermal analysis data as a measurement of the T_g of a confined film, because contact with the probe could confine molecular motion at the free surface. It is our assertion that the structure of the glass, and thus the T_g, is not influenced by probe contact while the probe temperature is below the T_g of the film. The glasses were prepared in the absence of the probe, and the conventional definition of polymer glass is that the time scales for structural relaxations are long relative to the time scale of the experimental observation. In molecular liquids near T_g, it may take minutes or hours for a molecule less than 10 Å in diameter to reorient.[6] Since the experiments were performed by heating the probe from room temperature to T_g, it is probable that the polymer chains at the surface are not influenced by the presence of the probe during the temperature ramp. Thus, the possibility that the experiments represent a measurement of the T_g of a confined film is unlikely, considering the time scales in the experiment.

As mentioned previously, a surprising outcome in this work is that the results from ellipsometry and local thermal analysis agree quantitatively. Ellipsometry analysis is performed with uniform heating of the film. Assuming the optical properties are not dependent on depth, ellipsometry measures an average property over the film thickness and is not sensitive to a thin surface layer of the film as in local thermal analysis. The fact that ellipsometry and local thermal analysis results compare quantitatively suggests that the glass transition temperature near the surface of a supported film is the same as the average T_g across the thickness of the film. These results appear to contrast with studies of surface molecular motion by Satomi et al.[13] Note, however, that local thermal analysis probes the top ~10% of a polymer film. It is possible that the surface T_g reported by Satomi et al. (by SVM measurement) is different from those reported here because the region of the film probed by the two techniques is different. It is difficult to make direct comparisons with the SVM results because the surface T_g reported in that work (ref 13) corresponded to relatively thick films (200 nm); no study of T_g with thickness was presented.

For thin enough films, the effects of film thickness on T_g, caused by either the presence of the free surface or the substrate, propagate throughout the film. Since for the systems studied here the film thickness at which the influence first occurs is approximately 45 nm, greater than the R_g of the polymer molecule (for PS M_w = 382 kg/mol, R_g = 19 nm; PMMA M_w = 100 kg/mol, R_g = 6 nm),[34] one could invoke collective molecular motion within the polymer glass as an explanation for the agreement between the data from the two methods. Note that the length scales commonly associated with heterogeneities as T_g is approached are relatively small (3 nm at $T = T_g + 10$ K in poly(vinyl acetate))[35] compared to the film thickness at which the T_g begins to deviate from the bulk value. However, it is possible that the range of correlated motion and the scale of dynamic heterogeneities are perturbed by confinement to thin films.

Conclusions

Local thermal analysis was developed as a convenient and effective technique to measure the glass transition temperature (T_g) of thin polymer films. We measured the T_g for polystyrene (PS) and poly(methyl methacrylate) (PMMA) films as a function of thickness for two different substrates, SiO_x and SiO_x treated with hexamethyldisilizane (HMDS). The T_g of PMMA and PS departed from the bulk value in films less than 45 nm thick. The T_g of PS decreased with similar magnitude on either substrate of SiO_x or SiO_x with HMDS. The T_g of thin films of PMMA increased on substrates of SiO_x but decreased on SiO_x with HMDS. Results from local thermal analysis agreed quantitatively with those obtained using ellipsometry.

Acknowledgment. We thank Mark Ediger for his helpful comments. We also thank Peter Pianoto and Alan Deutchendorf for their help in setting up the ellipsometer and scanning probe microscope experiments. This work is supported by the Semiconductor Research Corporation (Contract #98LP452) and the NSF (CTS-9708944 and CTS-9901430). The Center for Nanotechnology (CNTech) at the University of Wisconsin—Madison is supported by the DARPA/ONR. The Synchrotron Radiation Center at the University of Wisconsin—Madison is operated under a NSF award.

References and Notes

(1) Ediger, M. D. *Annu. Rev. Phys. Chem*., in press.
(2) Rao, V.; Hutchinson, J.; Holl, S.; Langston, J.; Henderson, C.; Wheeler, D. R.; Cardinale, G.; O'Connell, D.; Goldsmith, J.; Bohland, J.; Taylor, G.; Sinta, R. *J. Vac. Sci. Technol. B* **1988**, *16*, 3722.
(3) Solak, H. H.; He, D.; Li, W.; Cerrina, F. *J. Vac. Sci. Technol. B* **1999**, *17*, 3052.
(4) Fryer, D. S.; Bollepali, S.; de Pablo, J. J.; Nealey, P. F. *J. Vac. Sci. Technol. B* **1999**, *17*, 3351.
(5) Reynolds, G. W.; Taylor, J. W. *J. Vac. Sci. Technol. B* **1999**, *17*, 334.
(6) Ediger, M. D. *J. Phys. Chem*. **1996**, *100*, 13200.
(7) Cicerone, M. T.; Ediger, M. D. *J. Chem. Phys*. **1996**, *104*, 7210.
(8) Cicerone, M. T.; Blackburn, F. R.; Ediger, M. D. *Macromolecules*. **1995**, *28*, 8224.
(9) Keddie, J. L.; Jones, R. A. L.; Cory, R. A. *Europhys. Lett*. **1994**, *27*, 59.
(10) Dutcher, J. R.; Forrest, J. A.; Dalnoki-Veress, K. *Abstr. Pap. Am. Chem. Soc*. **1998**, *215*, 276.
(11) DeMaggio, G. B.; Frieze, W. E.; Gidley, D. W.; Zhu, M.; Hristov, H. A.; Yee, A. F. *Phys. Rev. Lett*. **1997**, *78*, 1524.
(12) Forrest, J. A.; Svanberg, C.; Revesz, K.; Rodahl, M.; Torell, L. M.; Kasemo, B. *Phys. Rev. E* **1998**, *58*, R1226.
(13) Satomi, N.; Takahara, A.; Kajiyama, T. *Macromolecules* **1999**, *32*, 4474.
(14) Wallace, W. E.; Vanzanten, J. H.; Wu, W. L. *Phys. Rev. E*. **1995**, *52*, R3329.
(15) Frank, B.; Gast, A. P.; Russell, T. P.; Brown, H. R.; Hawker, C. *Macromolecules* **1996**, *29*, 6531.
(16) Zheng, X.; Rafailovich, M. H.; Sokolov, J.; Strzhemechny, Y.; Schwarz, S. A.; Sauer, B. B.; Rubinstein, M. *Phys. Rev. Lett*. **1997**, *79*, 241.
(17) Keddie, J. L.; Jones, R. A. L.; Cory, R. A. *Faraday Discuss*. **1994**, 219.
(18) Kahle, O.; Wielsch, U.; Metzner, H.; Bauer, J.; Uhlig, C.; Zawatzki, C. *Thin Solid Films* **1988**, *313*, 803.
(19) Jiang, Q.; Shi, H. X.; Li, J. C. *Thin Solid Films* **1999**, *354*, 283.
(20) Forrest, J. A.; Mattsson, J. *Phys. Rev. E*. **2000**, *61*, R53.
(21) Torres, J. A.; Nealey, P. F., de Pablo, J. J., submitted to *Phys. Rev. Lett*.
(22) Fryer, D. S.; Kim, E. J.; Peters, R. D.; de Pablo, J. J.; Nealey, P. F.; White, C.; Wu, W., manuscript in preparation.
(23) Nealey, P. F.; Cohen, R. E.; Argon, A. S. *Macromolecules* **1994**, *27*. 4193.
(24) Breuer, H.; Rehage, G. *Kolloid-Z*. **1967**, *216/217*.
(25) Paniez, P. J.; Varielle, A.; Ballet, P.; Mortini, B. *Proc. SPIE*. **1998**, *3333*, 289.
(26) Pavelcheck, E. K.; Calabrese, G. S.; Dudley, B. W.; Jones, S. K.; Freeman, P. W.; Bohland, J. F.; Sinta, R. *Proc. SPIE* **1993**, *1925*, 264.
(27) Gomes, S.; Trannoy, N.; Grossel, P. *Meas. Sci. Technol*. **1999**, *10*, 805.
(28) Van Krevelen, D. W.; Hoftyzer, P. J. *Properties of Polymer*; Elsevier Scientific Publishing Company: Amsterdam, 1976.
(29) Bird, R. B.; Stewart, W. E.; Lightfoot, E. N. *Transport Phenomena*; John Wiley & Sons: New York, 1960.
(30) Hammiche, A.; Hourston, D. J.; Pollock, H. M.; Reading, M.; Song, M. *J. Vac. Sci. Technol. B* **1996**, *14*, 1486.
(31) Gomes, S.; Depasse, F.; Grossel, P. *J. Phys. D: Appl. Phys*. **1998**, *31*, 2377.
(32) Bandrup, J.; Imergut, E. H.; Grulke, E. A. *Polymer Handbook*; John Wiley & Sons: New York, 1998.
(33) Tye, R. P. *Thermal Conductivity*; Academic Press: London, 1969.
(34) Hiemenz, P. C. *Polymer Chemistry*; Marcel Dekker Inc.: New York, 1984.
(35) Tracht, U.; Wilhelm, H.; Heuer, A.; Spiess, H. W. *J. Magn. Reson*. **1999**, *140*, 460.

MA0003349